

Ensemble weather forecast post-processing with a flexible probabilistic neural network approach

Peter Mlakar^{1,2,3}, Janko Merše^{2,4}, and Jana Faganeli Pucer^{1,5}

¹University of Ljubljana, Faculty of Computer and Information Science, Slovenia

²Slovenian Environment Agency, Slovenia

³pm4824@student.uni-lj.si

⁴janko.merse@gov.si

⁵jana.faganeli@fri.uni-lj.si

ABSTRACT

Ensemble forecast post-processing is a necessary step in producing accurate probabilistic forecasts. Conventional post-processing methods operate by estimating the parameters of a parametric distribution, frequently on a per-location or per-lead-time basis. We propose a novel, neural network-based method, which produces forecasts for all locations and lead times, jointly. To relax the distributional assumption of many post-processing methods, our approach incorporates normalizing flows as flexible parametric distribution estimators. This enables us to model varying forecast distributions in a mathematically exact way. We demonstrate the effectiveness of our method in the context of the EUPPBench benchmark, where we conduct temperature forecast post-processing for stations in a sub-region of western Europe. We show that our novel method exhibits state-of-the-art performance on the benchmark, outclassing our previous, well-performing entry. Additionally, by providing a detailed comparison of three variants of our novel post-processing method, we elucidate the reasons why our method outperforms per-lead-time-based approaches and approaches with distributional assumptions.

Introduction

Forecast post-processing is a crucial task when constructing skillful weather forecasts. This is due to the inherent biases of the numerical weather predictions (NWP) which are the results of initial condition errors, computational simplifications, and sub-grid parametrizations [3, 20, 40]. All these factors combine and result in errors which are enhanced as the forecast horizon increases. Therefore, due to these issues, the forecast is uncertain by nature. To quantify this uncertainty ensemble forecasts are issued by centers for weather forecasts, such as the European Center for Medium Range Weather Forecasts (ECMWF) [13]. ECMWF generates these forecasts by perturbing the initial atmospheric conditions and varying the model parametrizations. This results in 50 different ensemble members, each expressing a potentially unique future weather situation. However, biases are still present in ensemble forecasts resulting in a disconnect between the specific observations and the described ensemble distribution.

Post-processing techniques are frequently employed by forecast providers [40] to mitigate the effects of biases in forecasts with the aim of constructing calibrated forecast probability distributions [16]. These techniques employ statistical approaches to map input ensemble forecasts to concur with actual weather variable observations. Techniques vary from simple to complex, from rigid [15, 31, 33, 37] to flexible [23, 26, 30, 39], and encompass a large spectra of statistical approaches [40]. Another way of distinguishing between post-processing methods is to characterize them based on their distributional assumptions or lack thereof. Since the nature of ensemble forecasts is inherently probabilistic (ensemble forecasts quantify the weather forecast uncertainty) the post-processing output should reflect that. Methods that assume the target weather variable distribution are usually simpler to implement however, they suffer from the pitfall of assuming the wrong distribution. This can result in additional biases. Likewise, different weather variables can exhibit different distributions therefore, tuning and exploration of the best target distribution is required before constructing the model. Methods that do not make such assumptions are frequently more complex to implement and require more data for parameter estimation.

Recently neural networks started showing promising results in this field [6, 7, 11, 17, 19, 28, 29, 29, 34, 35, 36, 41]. Applications such as those by Rasp and Lerch [34] exhibited state of the art results compared to conventional post-processing techniques. By using the ensemble mean and variance with the combination of station embeddings Rasp and Lerch [34] construct a neural network that estimates the parameters of a Gaussian distribution for each lead time. This approach is further extended in [36] by applying different distribution estimators in place of the normal distribution. To be more specific, they apply the same neural network architecture as a parameter predictor to three different models: a distributional regression model,

a Bernstein quantile regression model [6], and a histogram estimation model. Indeed, their aim to reduce the distributional assumption is apparent and also required as many weather variables can not be effectively described using simple probability distributions. We can make a similar observation by investigating the work by Veldkamp et al. [41] where the authors construct a convolutional neural network for post-processing wind speeds. Similarly to Schulz and Lerch [36], they tried different probability models as the output of their convolutional neural network: a quantized softmax approach, kernel mixture networks [1], and truncated normal distribution fitting approach. Veldkamp et al. [41] concluded that the most flexible distribution assessment method exhibited the best performance. This further bolsters the need for sophisticated distribution estimation techniques as these increase the performance of post-processing algorithms.

To further improve upon the existing post-processing techniques we propose two novel neural network approaches, Atmosphere NETwork 1 (ANET1) and Atmosphere NETwork 2 (ANET2). The novelty of the ANET methods is twofold and can be summarized thusly:

- Two novel neural network architectures for post-processing ensemble weather forecasts
- Joint probabilistic forecasting for all lead times and locations
- Flexible parametric distribution estimator based on normalizing spline flows [12], ANET2

Both ANET variants are constructed such that there is only one model for the entire post-processing region and all lead times. This is often not the case with frequently used post-processing methods [8] which typically construct individual models per-lead-time and sometimes even per-station. We show that our joint location-lead-time method ANET1 exhibits state-of-the-art performance on the EUPPBench benchmark [8] compared to other submitted methods, which are implemented on a per-lead time or per station basis.

ANET2 is the second iteration of our post-processing approach. ANET2 features an optimized neural network architecture, more in line with Rasp and Lerch [34], and training procedure compared to ANET1. Furthermore, ANET2 improves upon ANET1 by relaxing the distribution assumption of ANET1, which assumes that the target weather variable is distributed according to a parametric distribution which, in the case of temperature, is a normal distribution. ANET2 relaxes this assumption by modeling the target distribution in terms of a normalizing flow [9, 12, 24, 27]. This enables us to model mathematically exact distributions without specifying a concrete target distribution family. We demonstrate that ANET2 further improves upon ANET1 in a suite of performance metrics tailored for probabilistic forecast evaluation. Additionally, we provide intuition as to why such a type of joint forecasting and model construction leads to better performance by analyzing the feature importance encoded by the ANET2 model.

To demonstrate the performance of the ANET variants we compare four different novel methods for probabilistic post-processing of ensemble temperature forecasts. The first is ANET1. This method achieved state-of-the-art performance on the EUPPBench benchmark. The second is ANET2, our next version of ANET. It boasts a redesigned neural network architecture for parameter estimation and a flexible parametric distribution estimation model based on conditional normalizing flows. Third is ANET2_{NORM} which borrows the neural network architecture from ANET2 to estimate the parameters of a normal distribution to predict the future temperature uncertainty. Lastly, ANET2_{BERN} also borrows the neural network architecture from ANET2, however, it conducts distribution estimation using the popular quantile regression technique based on Bernstein polynomials, as described by Bremnes [6]. The Bernstein quantile regression technique was used previously for weather forecasts post-processing with good results [17, 36] and is therefore a natural candidate for this comparison. We describe our methods in more detail in the following sections. We evaluated of the aforementioned methods on the EUPPBench test dataset (referred to as D_{51}), focusing on post-processing temperature forecasts for stations in a subset of the European region (for more information refer to [8]).

Results

In this Section we present the evaluation of ANET1, ANET2, ANET2_{NORM}, ANET2_{BERN} on the D_{51} test dataset. We evaluate the performance of the above methods using the continuous ranked probability score (CRPS) [16], bias, quantile loss (QL), and quantile skill score (QSS) [6]. This evaluation is displayed in Figure 1 and Table 1. In the case of QSS, we use ANET1 as the reference model, quantifying the performance gain of ANET2 variants relative to ANET1. We compute the CRPS and bias by averaging them across all stations and time samples, resulting in a per-lead-time performance report. The performance values in Table 1 are a result of averaging the corresponding metrics across the entire test dataset.

Impact of improved network architecture and training procedure

To quantify the contributions of the ANET2 neural network architecture and training procedure, we look at the performance differences between ANET1 and the ANET2 variants. All ANET2 variants perform better on average than ANET1 across all

lead times in terms of CRPS and QSS. The difference between individual ANET2 variants is smaller, with ANET2 leading the pack. We notice that ANET2_{NORM} constantly outperforms ANET1 both in terms of average CRPS and QSS, which is further corroborated by the results in Table 1. However, both predict the same target distribution, that being the normal distribution. We attribute these performance differences to the architecture and training protocol changes, where the former has the bigger impact of the two. ANET2_{NORM} also exhibits the lowest bias amongst all methods. This could be due to the symmetric nature of the target normal distribution ANET2_{NORM}. Therefore, erroneous forecasts more easily incur similar penalties when spread around the mean, facilitating less bias in certain cases. Conversely, ANET1 outputs the same distribution as ANET2_{NORM} but has a higher bias. We believe that this difference is due to the less stable and less aligned training procedure of ANET1, which results in sub-optimal results.

Forecast calibration

To further quantify the probabilistic calibration of individual methods we use rank histograms [21], displayed in Figure 2. The results are aggregated across all stations, time samples, and lead times, for each quantile. This gives us an estimate of how well the individual methods describe the distribution of the entire D_{51} dataset. ANET1 and ANET2_{NORM} exhibit similar rank histograms due to both using a normal distribution as the target, resulting in similar deficiencies. The standout models are ANET2, which uses the modified normalizing flow approach, and ANET2_{BERN}, which is based on Bernstein polynomial quantile regression. Both methods are much more uniform compared to the remaining alternatives. For example, ANET2_{NORM} and ANET1 seem to suffer from over-dispersion as is implied by the hump between the 20-th and 40-th quantiles. We can observe similar phenomena with other post-processing methods that fit a normal distribution to temperature forecasts [8]. ANET2 and ANET2_{BERN} do not exhibit this specific over-dispersion, albeit with a small over-dispersion between the 10-th and 30-th quantile. Additionally, both methods under-predict upper quantiles, albeit to a lesser degree than ANET1 and ANET2_{NORM}. We also found that the ANET2_{BERN} method exhibits artefacts that are most pronounced at the low and high quantiles. We believe that this is due to the nature of the Bernstein quantile regression method where the fixed degree of the polynomial affects its expressive value, especially on the quantile edges. Overall, ANET2 displays the most uniform rank histogram compared to the remaining methods.

Per-altitude and per-station performance

Station altitude correlates with the decrease in model predictive performance, as we show in Figure 4. Therefore, we investigate the altitude-related performance of each model in terms of QSS over three station altitude intervals: $(-5, 800]$, $(800, 2000]$, and $(2000, 3600)$, displayed in Figure 3. We compute the per-altitude QSS by aggregating stations whose altitudes fall into a specific interval. Then we average the QL across all lead times, time samples, and corresponding stations, producing the QL on a per-quantile level. We use ANET1 as the reference model for the QSS. Looking at Figure 3, we can see that all ANET2 variants improve upon ANET1. The only exceptions are ANET2_{BERN} and ANET2_{NORM} that exhibit roughly equal QL for certain quantile levels at the altitude intervals $(-5, 800]$ and $(2000, 3600)$ respectively. ANET2 exhibiting the highest QSS of all methods. Indeed, ANET2 outperforms all the remaining methods over all quantile levels and all altitudes, with the exception of lower quantile levels at the stations with the lowest altitude where ANET2_{NORM} performs the best. The closest method, exhibiting similar trends in improvement to ANET2, is ANET2_{BERN}. In our opinion this and the results shown in Figure 2 further bolster the need for flexible distribution estimators. Similarly, by observing the average CRPS ranking per station, shown in Figure 4, we can see that ANET2 exhibits the best CRPS across 204 stations from a total of 229 stations. ANET2_{BERN} is the most performant method at 18 stations, with ANET2_{NORM} leading in CRPS only at 7 locations. ANET1 is not displayed as its CRPS does not outperform any of the ANET2 variants at any station.

	CRPS	Bias	QL
ANET2 _{NORM}	0.940	0.038	0.373
ANET2 _{BERN}	0.935	0.076	0.367
ANET2	0.923	0.069	0.363
ANET1	0.988	0.092	0.386

Table 1. CRPS, bias, and QL (quantile loss) for all evaluated methods averaged over all stations, time samples, and lead times for the D_{51} test dataset. The values in bold represent the best results for each metric.

Discussion

The results we presented provide a clear argument for the use of neural networks in conjunction with flexible distribution estimation methods. Even in the case of the initial run of the EUPPBench dataset with a limited number of predictors and one

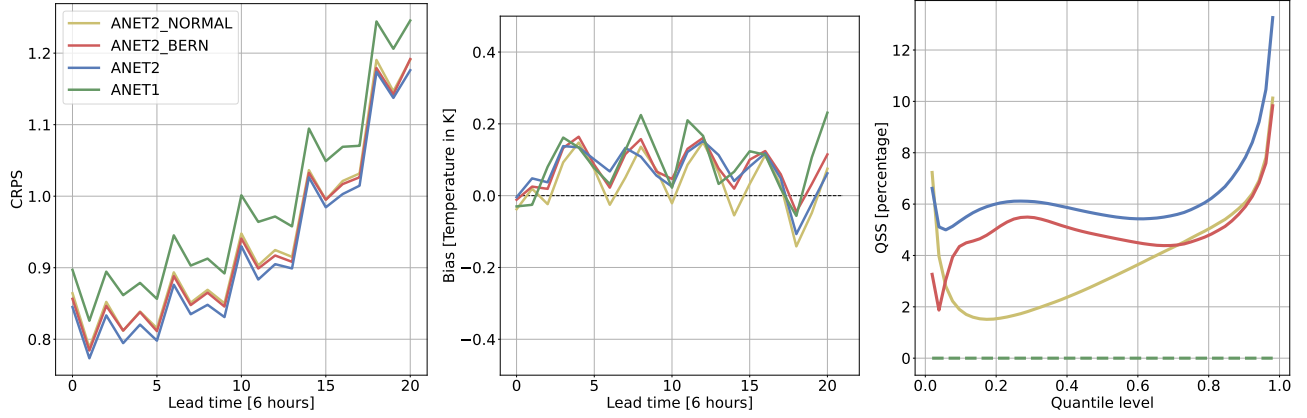


Figure 1. The CRPS, bias, and QSS for all ANET variants. A lower CRPS is better, a bias value closer to zero is better, and a higher QSS is preferable.

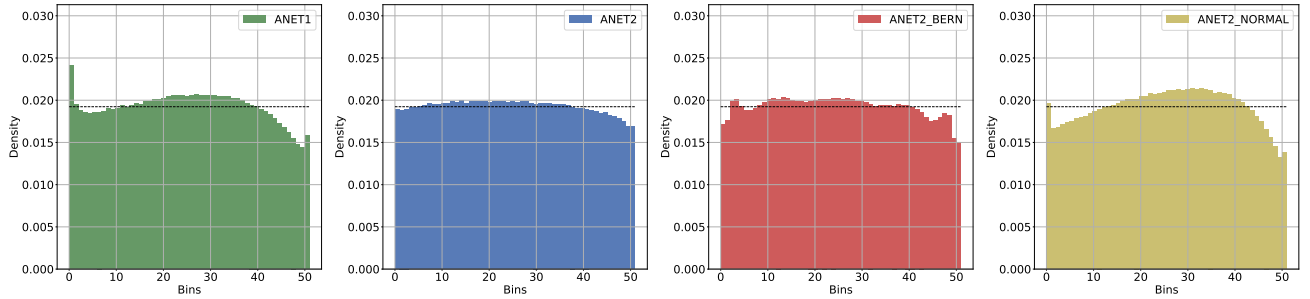


Figure 2. The rank histogram of all ANET variants. A more uniform histogram (column heights closer to the black dashed line) is better. Histograms with central humps imply over-dispersion while histograms with outliers on the edges represent under-dispersion.

target variable, neural networks can tangibly increase the state-of-the-art performance in post-processing. The comparative study we conducted between ANET1, the improved ANET2, and its variants, reveals useful guidelines for future method research and development.

ANET1 versus ANET2

First, our results corroborate the findings and practices outlined by Rasp and Lerch [34]. ANET1 uses a per-ensemble-member dynamic attention mechanism with the idea of determining the individual ensemble member importance, conditioned on the predictors and weather situation. While the idea is sound in our opinion, further testing with ANET2 revealed that performing regression on the ensemble mean and variance resulted in equal or even slightly better performance, with a similar number of model parameters. We also evaluated the effects of including additional statistics, such as the minimal and maximal temperature, and median temperature. We found that these do not impact the model’s predictive performance. Therefore, we conclude that for the EUPPBench dataset v1.0, it seems that the ensemble statistics such as mean and variance contain enough information for the formation of skillful probabilistic forecasts of temperature. However, it likely that we have not yet found an efficient way to extract information from individual ensemble members.

ANET2 versus ANET2_{NORM} and ANET2_{BERN}

ANET2_{NORM} operates by assuming the target weather distribution. However, this method is outperformed by the remaining two, more flexible methods when observing the mean QSS and CRPS. Similar observations were found by other researchers [37, 41] further underlining the need for flexible distribution estimators. From the two flexible approaches we implemented, ANET2 outperforms ANET2_{BERN} in all metrics. The ability to model the probability density through a cascade of spline transformations seems to offer greater flexibility compared to the Bernstein polynomial approach. Additionally, ANET2 does not suffer from the quantile crossing issue that can occur with Bernstein quantile regression [6]. ANET2 produces a probabilistic model from which we can estimate the exact density, distribution, and samples from the distribution.

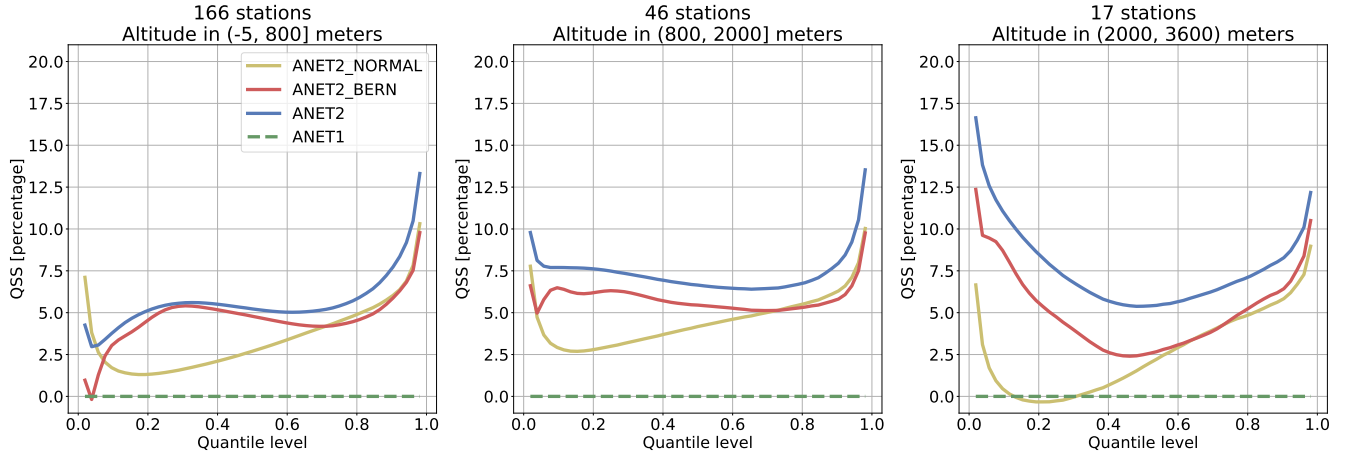


Figure 3. QSS for all compared methods relative to stations with different altitudes. ANET1 is used as the reference model, therefore, the y-axis denotes the percentage improvement compared to ANET1.

Joint lead time forecasting

Where we believe that ANET2 and ANET1 innovate compared to previously applied neural network approaches is in the post-processed forecast lead time. All ANET variants perform predictions for the entire lead time. They are single models for all lead times and all stations, taking as input the entire ensemble forecast (whole lead time). This enables ANET to model dependencies between different forecast times. These ideas are further corroborated by investigating the feature importance generated using input feature permutation [14]. We investigate how different lead times in the input help form the post-processed output for other lead times.

We display the input variable importance relative to a target lead time in Figure 5. Each row signifies a specific lead time in the post-processing output while a column denotes a specific lead time in the ensemble forecast that forms the model input. In many cases, off diagonal elements of each row exhibit high importance implying that ensemble forecasts for different lead times contribute to the correction for a specific target lead time. For example, when ANET2 predicts the distribution for the first target lead time (row denoted with zero) it heavily relies on the first three input forecast lead times (the first three columns). We can also observe that past forecasts exhibit higher importance compared to future forecasts, relative to a specific target lead time. This is implied by the darker lower triangle of the importance matrix (area under the blue dashed line). Likewise, we can identify an interesting, periodic trend when observing the columns corresponding to lead times at noon. We can see that these forecasts non-trivially impact post-processing any target lead time. We hypothesise that this is due to the daily temperature, which frequently reaches its maximum value at noon (this is due to the six-hour resolution), playing an important role in the amount of heat retained throughout the night (void of all other predictors). Since the first noon forecast is the most accurate compared to the rest it acts as an estimator, with consecutive noon forecasts decreasing in importance due to forecast errors.

Additionally, looking at the CRPS comparison of ANET1 with other state-of-the-art post-processing techniques evaluate on the EUPPBench dataset (page 17, Figure 3 ion [8]) we can observe that ANET1 exhibits better correction for temperatures at midnight. The remaining methods suffer from stronger periodic spikes in error when post-processing those lead times. However, the majority of the implemented methods in [8] (except for reliance calibration) operate on a single lead time. If we turn our attention again to Figure 5 and look at each labeled row (corresponding to midnight forecasts), we can see that the importance is more spread out between multiple input lead times. Therefore, it seems that information important for post-processing forecast at midnight is not solely concentrated at that time but is spread out. This might explain why our method can better suppress forecast errors at these lead times.

Modified derivative estimator

In this section we present our modification to the derivative estimator of ANET2’s distribution model which is based on normalizing spline flows [12]. The implementation described by Durkan et al. [12] requires the estimation of three sets of parameters for the spline transformations: spline knots, spline values at the knots, and spline derivatives at the knots. Durkan et al. [12] suggest that these parameters be estimated by a neural network. However, in our testing, this resulted in sharp discontinuities in the probability density of the final estimated distribution, as can be seen in Figure 6. This is because the values of the derivatives are selected independently of the knots and values, resulting in potential discontinuities. Durkan et al. [12] state that this induces multi-modality into the density. However, this might hamper future efforts for determining the most likely predicted weather outcome as sharp jumps in the density could introduce noise around the modes. To produce smoother

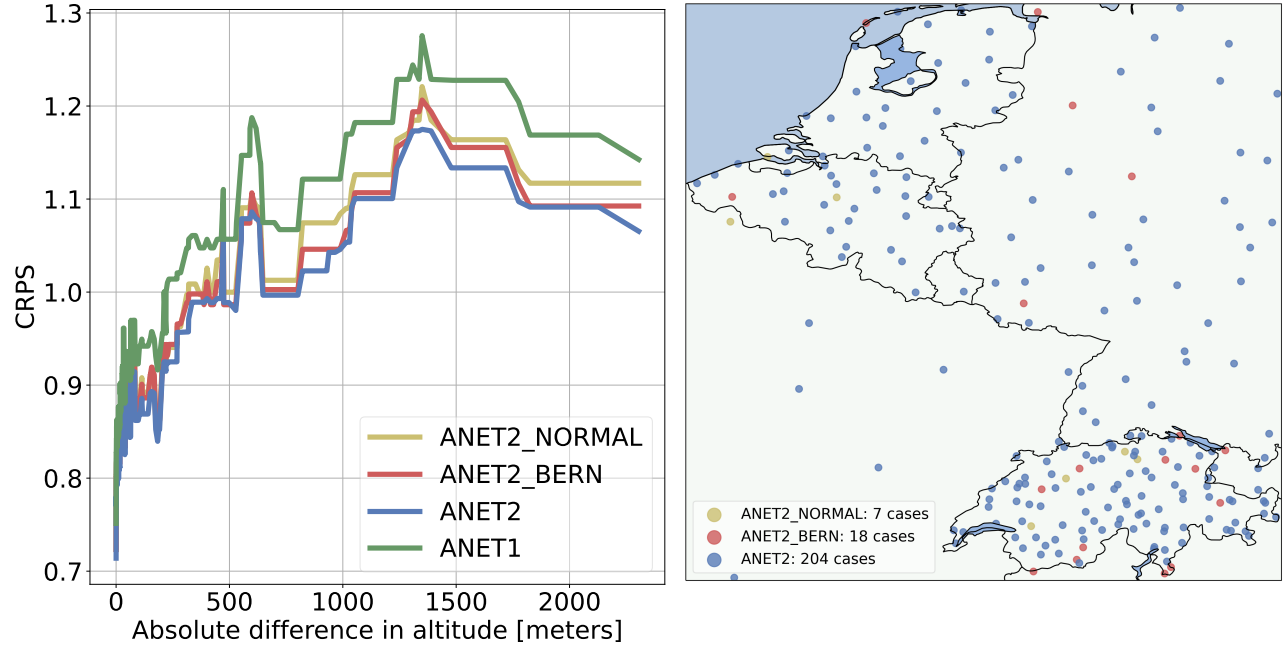


Figure 4. (Left): Average per-station CRPS relative to the absolute difference between the model and station altitude. We used median filtering with a kernel size of 15 to suppress outliers. An increase in CRPS correlates with an increase in the absolute difference in altitude. (Right): Average per-station CRPS. The number of cases in which a specific method outperformed the remaining is denoted in the legend. ANET1 is not displayed since it never performed better versus the ANET2 variants.

densities, we modified the derivative estimation procedure such that it now entirely depends on the spline knots and values. This modified derivative estimator was described by Gregory and Delbourgo [18] and offers certain spline continuity guarantees. The resulting probability density is much smoother (right panel in Figure 6) and in our tests, the modified distribution estimator performs equally well relative to the default derivative estimator in terms of predictive power in our test scenario.

Another positive attribute of the modified derivative estimation approach is the fact that it reduced the required number of parameters our neural network has to estimate by a third. This is because in our case the derivatives are estimated from the existing spline knots and values, while the default implementation required the explicit estimation of all three sets of parameters by the neural network. For example, ANET2 issues a probabilistic forecast for each lead time. If we use a normalizing spline flow with s consecutive spline transformations, each containing k knots, this results in $21 \times (s \times k \times 3)$ parameters for the default derivative estimation implementation (21 for each lead time, times s for each spline, times k for the number of knots, times 3 for each set of parameters - knots, values, derivatives). Contrary to that, the modified derivative approach requires $21 \times (s \times k \times 2)$ parameters, as the derivatives are estimated from the remaining parameters.

ANET2 drawbacks

The enhanced distributional flexibility of ANET2 comes with two drawbacks: an increased number of parameters in the distribution model, and increased execution time. The execution time and distribution model parameter count comparison is displayed in Table 2. We can see that ANET2 is the slowest of all three variants, exhibiting a roughly five times slower inference time for the D_{51} dataset compared to ANET2_{BERN}. ANET2_{NORM} has the lowest execution speed, followed by ANET2_{BERN}. This difference in time is mainly due to the sequential nature of the normalizing spline flow: input data has to first pass through a cascade of spline transformations before the density can be estimated. Additionally, when a data sample passes through a spline transformation it has to locate the appropriate spline bin or interval which incurs additional computational burdens of searching for that bin (Durkan et al. [12] suggest the use of bisection to speed up this search, however, we do not implement this procedure). The execution times are still small in an absolute sense, as all methods require less than a minute to post-process the entire D_{51} test dataset, which contains 167170 forecasts. Nevertheless, we must keep this in mind as these computational burdens might compound in a more complex setting with multiple forecast variables in a spatial context.

We can also see that ANET2 requires the highest number of parameters for determining the distribution model. Although ANET2 outperforms ANET2_{BERN} in all forecast evaluation metrics, we have reached the area of diminishing returns. ANET2 requires three times as many parameters compared to ANET2_{BERN} to produce these improvements.

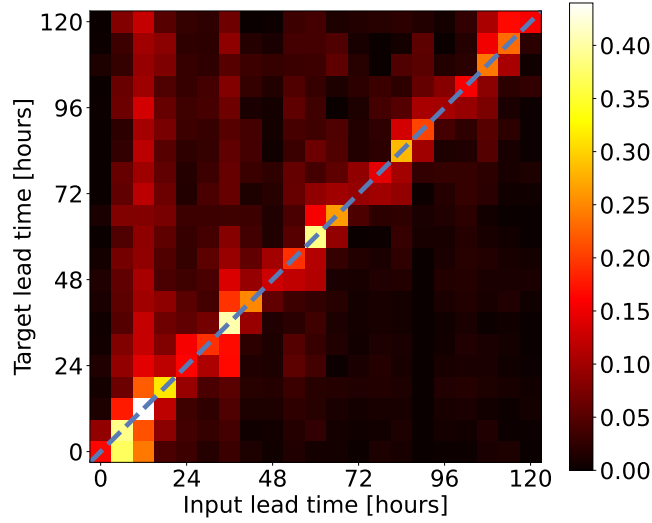


Figure 5. Input forecast lead times (x axis) importance relative to ANET2’s post-processed lead time outputs (y axis). Values on the diagonal (blue dashed line) represent the importance of each input lead time to its corresponding post-processed lead time output. Example: the column labeled 24 contains the importance measures of the forecast issued at that lead time on all lead times in the post-processed output.

Still, even in the face of these drawbacks, we believe that ANET2 is the most compelling of the three compared approaches in the EUPPBench setting due to its superior distribution estimation performance, and exact probability distribution estimation with no potential quantile crossing. Perhaps these would require attention in a more complex forecast post-processing scenario, however, this requires additional research and testing.

	Inference time for D_{51} test dataset	Number of parameters in distribution model
ANET2 _{NORM}	2.87 seconds	42
ANET2 _{BERN}	7.14 seconds	273
ANET2	36.08 seconds	840

Table 2. The inference execution times and the number of distributional model parameters required by each ANET2 variant. Values in bold are better. The inference times are produced with an Nvidia Quadro P400 graphics card on a system with an Intel i7 9700K processor with 32 gigabytes of memory.

Methods

ANET1

ANET1 is a neural network based approach for probabilistic ensemble forecast post-processing. The ANET1 architecture, displayed in Figure 7, is tailored for processing ensemble forecasts with a varying number of ensemble members. ANET1 achieves this by first processing ensemble forecasts for the entire lead time individually, by passing them through a shared forecast encoder structure. We concatenate per-station predictors to each ensemble forecast to allow ANET1 to adapt to individual station conditions. The predictors include station and model altitude, longitude, latitude, and land usage, with the addition of a seasonal time encoding, defined as $\cos(\frac{2\pi d}{365})$, where d denotes the day of year the individual input forecast was issued. The shared forecast encoder transforms each forecast-predictor pair into a high-dimensional latent encoding. The individual encodings are then weighed by a dynamic attention block and averaged into a single, mean ensemble encoding. This dynamic attention mechanism is designed to determine the importance of individual ensemble members in a given weather situation. This is one of the procedures that differentiate ANET1 from methods such as Rasp and Lerch [34] since individual ensemble member features are retained longer in the post-processing procedure. The mean ensemble encoding is then passed through a regression block, the outputs of which are the per lead time additive corrections to the ensemble mean and standard deviation. We use the corrected mean and standard deviation as parameters of the predictive normal distribution. The parameters

of the network were estimated using gradient descent by minimizing the negative log-likelihood of the predicted model.

ANET2

ANET1 suffers from the drawback of being restricted to the normal distribution as the predictive weather distribution. One solution is to fit other specific existing distributions to data based on expert knowledge of the best possible fit. However, more flexible methods tend to outperform these approaches [40]. To this end, we draw from normalizing spline flows [12]. These models are designed for density estimation and can approximate complex distributions in a tractable and mathematically exact way. However, as we require a conditional distribution estimator given a forecast, we have to modify the normalizing flow approach to fit our context.

Flexible parametric distribution estimation using modified normalizing flows

We define a rational-quadratic spline transformation $T(x; \theta)$, parameterized by θ , with x as the target temperature realization. The transformation T_θ is a strictly increasing and differentiable transformation. The parameter set θ includes the spline knots and the spline's values at those knots. Since our goal is to model the target temperature distribution F_{temp} we can use the change of variable approach [27] to express this unknown distribution in terms of the transformation T_θ and a base distribution F_{norm} , which is in our case a univariate normal distribution. The target variable density can then be defined as

$$p_{temp}(x; \theta) = p_{norm}(T_\theta(x)) \frac{\partial T_\theta(x)}{\partial x}.$$

Since p_{norm} is the density of a normal distribution with zero mean and standard deviation of one, the final loss function minimized (the negative log-likelihood) for a given sample x_i is

$$L(p_{temp}(x_i)) = \frac{T_\theta(x_i)^2}{2} - \ln\left(\frac{\partial T_\theta(x_i)}{\partial x}\right).$$

The transformation T_θ can be a composition of multiple rational-quadratic spline transformations. Therefore, the set of parameters θ encompasses the parameters of all sequential spline transformations. ANET2 uses a sequence of four rational quadratic spline transformations, each described by five knot-value pairs. We generate a distribution for each lead time. This means that the parametric distribution described by this model contains 840 parameters ($21 \times (10 \times 4)$: 21 for each lead time, 10 for each of the 4 spline transformations).

To fully describe a rational quadratic spline we require the spline's knot-value pairs and the value of the spline's derivative at those knots. The knot-value pairs are estimated by the ANET2 neural network (described in more detail in the following section). For a specific ensemble forecast with a lead time of t steps, ANET2 computes t parameter sets θ_l , where $l \in [1, t]$. Each θ_l is comprised of two vectors, the knots of the transformation and the values of the transformation at time l . More formally,

$$\theta_l := \{\mathbf{k}_l, \mathbf{v}_l\},$$

where the vector \mathbf{k}_l denotes the transformation knots and \mathbf{v}_l the values. We use a neural network to estimate these values. The monotonicity of the spline knot-value pairs is ensured using the softplus [10] function. Therefore, the final vector of knots \mathbf{k} and values \mathbf{v} for the forecast time l are defined as

$$\begin{aligned} \mathbf{k}_l &:= \text{CumSum}([\mathbf{k}'_{l,1}, 1e^{-3} + \text{Softplus}(\mathbf{k}'_{l,[2,5]})]), \\ \mathbf{v}_l &:= \text{CumSum}([\mathbf{v}'_{l,1}, 1e^{-3} + \text{Softplus}(\mathbf{v}'_{l,[2,5]})]), \end{aligned}$$

where \mathbf{k}'_l and \mathbf{v}'_l refer to the raw neural network outputs for the knot-value pairs, $\mathbf{k}'_{l,1}$ refers to the first element of the vector \mathbf{k}'_l , while $\mathbf{k}'_{l,[2,5]}$ contains all elements of the vector but the first (the same holds true for \mathbf{v}'_l). The index into \mathbf{k}' and \mathbf{v}' goes up to five we only have five knot-value pairs per spline. Additionally, we limit the minimal distance between two consecutive knot-value pairs to be $1e^{-3}$. This is done to ensure numerical stability and in our testing does not impact the regression performance. The function CumSum denotes the cumulative sum operation, where the first element is kept identical. This ensures that the knots-value pairs increase monotonically, guaranteeing the monotonicity of the rational quadratic spline transformation [18].

However, to provide a full estimate of the transformation we also require the positive derivative values at the knots. Durkan et al. [12] propose that we determine these derivatives from the neural network in much the same way as the knot-value pairs. This definition of the derivative can yield discontinuities in the splines and therefore in the final estimated density. This is not practical for our application context as we frequently inspect the probability density to determine the most likely weather outcome. A density full of discontinuities conveys unnatural properties and impedes the required analysis. To rectify this we

look at the work by Gregory and Delbourgo [18], where they propose a derivative estimation schema that computes the required derivatives from the knot-value pairs. It is this derivative estimation approach that we adopt in our work.

Likewise, we do not restrict the spline knots to a predetermined interval. This is contrary to Durkan et al. [12], however, in our testing, this works well and provides no tangible difference in performance. It does, however, eliminate the need for parameter tuning as the knot ranges are determined automatically during optimization.

We estimate the parameter values of the spline transformations using gradient descent by minimizing the negative log-likelihood of the distribution model.

Parameter estimation neural network architecture

To determine the values of these spline parameters (in the case of ANET2_{NORM} the parameters of a normal distribution and in the case of ANET2_{BERN} the coefficients of the Bernstein polynomial) we use a dense neural network, whose architecture is displayed in Figure 8. ANET2 conducts post-processing jointly for the whole lead time and all spatial locations. Therefore, the input to the network is an ensemble forecast with m ensemble members, each containing 21 forecasts (we will discuss the training dataset and training procedure in the following section). ANET2 first computes the ensemble forecast mean and variance. These two vectors, each containing 21 elements, are then concatenated with the per-station predictors and seasonal time encodings to form the input to the neural network. The per-station predictors include station and model altitude, longitude, latitude, and land usage. The seasonal time encoding is defined as $\cos(\frac{2\pi d}{365})$, where d denotes the day of year the forecast was issued. There are a total of six dense layers in the ANET2 neural network. All dense layers, except for the last one, are followed by a SiLU [22] activation, and each of the layers, except for the first and last, are preceded by a dropout layer [38] with a dropout probability of 0.2. Each of these dense layers is a residual layer implying that the transformation done by the dense layer and the consequent activation is added to the input of that layer, which then forms the output of that residual block (inspect Figure 8 for more details). The final layer produces 21 sets of parameters θ , representing the parametric distribution for each forecast time.

ANET2_{NORM}

ANET2_{NORM} combines the ANET2 neural network model described above with a normal distribution acting as its probability distribution model. Therefore, we model the mean and standard deviation vectors of the distribution, each containing 21 values corresponding to the forecast times. Let us denote the raw ensemble mean and standard deviation vectors as μ^e, σ^e . We compute the final model mean and standard deviation vectors μ, σ as

$$\mu = \mu^e + \mu', \quad (1)$$

$$\sigma = \sigma^e + \text{Softplus}(\sigma'), \quad (2)$$

where μ', σ' denote the raw neural network estimates for those parameters. We again use the Softplus function to enforce the positivity constraint on the standard deviation. We found that if we use the neural network to predict the mean and standard deviation correction residual (expressed as an additive correction term to the raw ensemble statistics) the model performs better than it would if it were to directly predict the target mean and standard deviation without the residual. The model is trained by minimizing the negative log-likelihood loss.

ANET2_{BERN}

Similarly to ANET2_{NORM}, we form ANET2_{BERN} by combining the neural network parameter estimation architecture of ANET2 with the quantile regression framework described by Bremnes [6] as its probability distribution model. In this case, the output of the neural network model is a set of 21 Bernstein polynomial coefficient vectors, each containing 13 values. Therefore, the degree of the Bernstein polynomial we fit is 12 (the degree is one less than the number of parameters). As per the suggestion of Bremnes [6] we train the model by minimizing the quantile loss on 100 equidistant quantiles. To ensure that no quantile crossing can occur, Bremnes [6] suggest one might restrict the polynomial coefficient to the positive reals. However, in our testing, this limits the expressive power of the model. Therefore, we let the coefficients be unconstrained as the quantile crossing event is rare in practice [6] and we did not encounter it in our testing (however, one must not neglect this correctness concession as it can be a source of potential issues if left unchecked).

Training procedure

The training procedure is different between ANET1 and the remaining ANET2 variants. The reason for this discrepancy was the fact that ANET1 preceded ANET2 in development. We describe both approaches and give our arguments as to why we modified the training procedure.

In both cases, we used the datasets provided by the EUPPBench benchmark [8] to construct the model. The pilot study focused on the post-processing of temperature forecasts for stations in a limited region in Europe. This study included two datasets. The first dataset, denoted as D_{11} , consisted of 20 year re-forecasts [8] for the years 2017, 2018, with 209 time samples

for both years. The ensemble for this dataset counted 11 members. The D_{11} dataset was the designated training dataset. The second dataset, denoted as D_{51} , included forecasts for 2017, 2018, with 730 time samples for both years. The ensemble for this dataset counted 51 members. The D_{51} dataset was the designated test dataset. We performed post-processing for 229 stations which were equal for both datasets. Each training batch consisted of 256 randomly selected samples across all stations, years, and time samples.

The dataset described above and their designated use were equal across ANET1 and all the ANET2 variants. The main difference between the training procedures of ANET1 and the ANET2 variants lies in how we split the D_{11} dataset into the training and validation subsets.

ANET1 training procedure

To create the training-validation split we randomly partitioned the D_{11} dataset across all stations, years, and time samples. The first partition was the final training dataset subset, consisting of 80 percent of D_{11} . The remaining 20 percent formed the validation dataset. We select the model that exhibits the lowest validation loss as the final candidate model. Additionally, the model does not use the validation dataset for parameter estimation during training. This way we select the model that minimizes the unseen data loss in a particular training setup. The random partitioning required us to carefully evaluate early stopping conditions as it quickly lead to overfitting due to their distribution similarity. We use the Adam optimizer [25] in the Pytorch [32] framework with its default parameters, a batch size of 128 samples, learning rate of 10^{-3} , and weight decay of 10^{-9} . If the validation loss does not improve for more than 20 epochs the training is terminated. We reduce the learning rate by a factor of 0.9 after the validation loss plateaus for 10 epochs to increase numerical stability.

Even though ANET1 managed to perform well in the final evaluation, this set-up poorly reflected the nature of the train-test relationship. It also lead to stability issues. We rectified this in the next iteration of the training procedure.

ANET2 variants training procedure

To rectify the issues of the previous training approach we forwent the random split approach. Therefore, we formed the validation subset of D_{11} with the re-forecasts corresponding to the year 2016 while we used all the remaining data to train the model. This reflects the train-test dynamic of D_{11} and D_{51} , measuring the "out-of-sample" predictive power of the model, as the validation subset is not sampled from the same years as the training one. Similarly to ANET1, we select the model that exhibits the lowest validation loss as the final candidate model with the validation dataset not being used for parameter estimation during training. This way we select the model that minimizes the unseen data loss in a particular training setup. We use the Adam optimizer in the Pytorch framework with its default parameters, a batch size of 256 samples, learning rate of 10^{-3} , and weight decay of 10^{-6} . A bigger weight decay helps with the stability of the learning procedure as the method is more flexible than ANET1 and therefore requires additional regularization. Finally, we also reduce the learning rate by a factor of 0.9 after the validation loss plateaus for 10 epochs to increase numerical stability.

Data Availability

The data used in this study is part of the the EUPPBench dataset, which is available at [5]. However, a subset of stations used in this study is not publicly available. We refer the reader to [8] for more details with regards to the available dataset.

Code Availability

The ANET2 variants are open source and available at GitHub [2]. Likewise, the code for ANET1 is open source as well and available at GitHub [4].

References

1. Luca Ambrogioni, Umut Güçlü, Marcel A. J. van Gerven, and Eric Maris. The Kernel Mixture Network: A Nonparametric Method for Conditional Density Estimation of Continuous Random Variables, 2017. *_eprint*: 1705.07111.
2. ANET2, 2023-03-28. URL <https://github.com/petermlakar/ANET2>.
3. Peter Bauer, Alan Thorpe, and Gilbert Brunet. The quiet revolution of numerical weather prediction. *Nature*, 525 (7567):47–55, September 2015. ISSN 1476-4687. doi: 10.1038/nature14956. URL <https://doi.org/10.1038/nature14956>.
4. EUPP benchmark/ESSD ANET, 2023-03-28. URL <https://github.com/EUPP-benchmark/ESSD-ANET>.
5. Jonas Bhend, Markus Dabernig, Jonathan Demaeyer, Olivier Mestre, and Maxime Taillardat. EUPPBench postprocessing benchmark dataset - station data, March 2023. URL <https://doi.org/10.5281/zenodo.7708362>.

6. John Bjørnar Bremnes. Ensemble postprocessing using quantile function regression based on neural networks and Bernstein polynomials. *Monthly Weather Review*, 148(1):403–414, 2020. Publisher: American Meteorological Society.
7. William E Chapman, Luca Delle Monache, Stefano Alessandrini, Aneesh C Subramanian, F Martin Ralph, Shang-Ping Xie, Sebastian Lerch, and Negin Hayatbini. Probabilistic predictions from deterministic atmospheric river forecasts with deep learning. *Monthly Weather Review*, 150(1):215–234, 2022.
8. J. Demaeyer, J. Bhend, S. Lerch, C. Primo, B. Van Schaeybroeck, A. Atencia, Z. Ben Bouallègue, J. Chen, M. Dabernig, G. Evans, J. Faganeli Pucer, B. Hooper, N. Horat, D. Jobst, J. Merše, P. Mlakar, A. Möller, O. Mestre, M. Taillardat, and S. Vannitsem. The EUPPBench postprocessing benchmark dataset v1.0. *Earth System Science Data Discussions*, 2023:1–25, 2023. doi: 10.5194/essd-2022-465. URL <https://essd.copernicus.org/preprints/essd-2022-465/>.
9. Laurent Dinh, Jascha Sohl-Dickstein, and Samy Bengio. Density estimation using real nvp. *arXiv preprint arXiv:1605.08803*, 2016.
10. Softplus — PyTorch 2.0 documentation, 2023-03-28. URL <https://pytorch.org/docs/stable/generated/torch.nn.Softplus.html>.
11. Florian Dupuy, Olivier Mestre, Mathieu Serrurier, Valentin Kivachuk Burdá, Michaël Zamo, Naty Citlali Cabrera-Gutiérrez, Mohamed Chafik Bakkay, Jean-Christophe Jouhaud, Maud-Alix Mader, and Guillaume Oller. ARPEGE Cloud Cover Forecast Postprocessing with Convolutional Neural Network. *Weather and Forecasting*, 36(2):567 – 586, 2021. doi: <https://doi.org/10.1175/WAF-D-20-0093.1>. URL <https://journals.ametsoc.org/view/journals/wefo/36/2/WAF-D-20-0093.1.xml>. Place: Boston MA, USA Publisher: American Meteorological Society.
12. Conor Durkan, Artur Bekasov, Iain Murray, and George Papamakarios. Neural spline flows. *Advances in neural information processing systems*, 32, 2019.
13. ECMWF. <https://www.ecmwf.int/en/forecasts>, 2022.
14. Aaron Fisher, Cynthia Rudin, and Francesca Dominici. All Models are Wrong, but Many are Useful: Learning a Variable’s Importance by Studying an Entire Class of Prediction Models Simultaneously. *Journal of Machine Learning Research*, 20(177):1–81, 2019. URL <http://jmlr.org/papers/v20/18-760.html>.
15. Tilmann Gneiting, Adrian E. Raftery, Anton H. Westveld, and Tom Goldman. Calibrated probabilistic forecasting using ensemble model output statistics and minimum CRPS estimation. *Monthly Weather Review*, 133(5), 2005. doi: 10.1175/MWR2904.1.
16. Tilmann Gneiting, Fadoua Balabdaoui, and Adrian E. Raftery. Probabilistic forecasts, calibration and sharpness. *Journal of the Royal Statistical Society. Series B: Statistical Methodology*, 69(2), 2007. doi: 10.1111/j.1467-9868.2007.00587.x.
17. Tilmann Gneiting, Sebastian Lerch, and Benedikt Schulz. Probabilistic solar forecasting: Benchmarks, post-processing, verification. *Solar Energy*, 252:72–80, 2023. ISSN 0038-092X. doi: <https://doi.org/10.1016/j.solener.2022.12.054>. URL <https://www.sciencedirect.com/science/article/pii/S0038092X22009343>.
18. J. A. Gregory and R. Delbourgo. Piecewise Rational Quadratic Interpolation to Monotonic Data. *IMA Journal of Numerical Analysis*, 2(2):123–130, April 1982. ISSN 0272-4979. doi: 10.1093/imanum/2.2.123. URL <https://doi.org/10.1093/imanum/2.2.123>. _eprint: <https://academic.oup.com/imanj/article-pdf/2/2/123/2267745/2-2-123.pdf>.
19. Peter Grönquist, Chengyuan Yao, Tal Ben-Nun, Nikoli Dryden, Peter Dueben, Shigang Li, and Torsten Hoefler. Deep learning for post-processing ensemble weather forecasts. *Philosophical Transactions of the Royal Society A: Mathematical, Physical and Engineering Sciences*, 379(2194):20200092, February 2021. doi: 10.1098/rsta.2020.0092. URL <https://doi.org/10.1098/rsta.2020.0092>. Publisher: Royal Society.
20. G.J. Hakim and J. Patoux. *Weather: A Concise Introduction*. Cambridge University Press, 2017. ISBN 978-1-108-40465-5. URL <https://books.google.si/books?id=pqXoAQAAAJ>.
21. Thomas M. Hamill. Interpretation of Rank Histograms for Verifying Ensemble Forecasts. *Monthly Weather Review*, 129(3):550 – 560, 2001. doi: 10.1175/1520-0493(2001)129<0550:IORHFV>2.0.CO;2. URL https://journals.ametsoc.org/view/journals/mwre/129/3/1520-0493_2001_129_0550_iorhfv_2.0.co_2.xml. Place: Boston MA, USA Publisher: American Meteorological Society.

22. Dan Hendrycks and Kevin Gimpel. Gaussian Error Linear Units (GELUs). *arXiv preprint arXiv:1606.08415*, 2023.
23. Timothy David Hewson and Fatima Maria Pillosu. A low-cost post-processing technique improves weather forecasts around the world. *Communications Earth & Environment*, 2(1):132, 2021. Publisher: Nature Publishing Group UK London.
24. Priyank Jaini, Ivan Kobyzev, Yaoliang Yu, and Marcus Brubaker. Tails of Lipschitz Triangular Flows. In Hal Daumé III and Aarti Singh, editors, *Proceedings of the 37th International Conference on Machine Learning*, volume 119 of *Proceedings of Machine Learning Research*, pages 4673–4681. PMLR, July 2020. URL <https://proceedings.mlr.press/v119/jaini20a.html>.
25. Diederik P. Kingma and Jimmy Ba. Adam: A Method for Stochastic Optimization. *arXiv preprint arXiv:1412.6980*, 2017.
26. Charlie Kirkwood, Theo Economou, Henry Odbert, and Nicolas Pugeault. A framework for probabilistic weather forecast post-processing across models and lead times using machine learning. *Philosophical Transactions of the Royal Society A*, 379(2194):20200099, 2021. Publisher: The Royal Society Publishing.
27. Ivan Kobyzev, Simon JD Prince, and Marcus A Brubaker. Normalizing flows: An introduction and review of current methods. *IEEE transactions on pattern analysis and machine intelligence*, 43(11):3964–3979, 2020. Publisher: IEEE.
28. Sebastian Lerch and Kai L Polsterer. Convolutional autoencoders for spatially-informed ensemble post-processing. *arXiv preprint arXiv:2204.05102*, 2022.
29. Amy McGovern, Kimberly L. Elmore, David John Gagne, Sue Ellen Haupt, Christopher D. Karstens, Ryan Lagerquist, Travis Smith, and John K. Williams. Using Artificial Intelligence to Improve Real-Time Decision-Making for High-Impact Weather. *Bulletin of the American Meteorological Society*, 98(10):2073 – 2090, 2017. doi: <https://doi.org/10.1175/BAMS-D-16-0123.1>. URL <https://journals.ametsoc.org/view/journals/bams/98/10/bams-d-16-0123.1.xml>. Place: Boston MA, USA Publisher: American Meteorological Society.
30. Annette Möller, Ludovica Spazzini, Daniel Kraus, Thomas Nagler, and Claudia Czado. Vine copula based post-processing of ensemble forecasts for temperature. *arXiv preprint arXiv:1811.02255*, 2018.
31. Kaleb Phipps, Sebastian Lerch, Maria Andersson, Ralf Mikut, Veit Hagenmeyer, and Nicole Ludwig. Evaluating ensemble post-processing for wind power forecasts. *Wind Energy*, 25(8):1379–1405, 2022. Publisher: Wiley Online Library.
32. PyTorch, 2023-03-28. URL <https://pytorch.org/>.
33. Adrian E. Raftery, Tilmann Gneiting, Fadoua Balabdaoui, and Michael Polakowski. Using Bayesian model averaging to calibrate forecast ensembles. *Monthly Weather Review*, 133(5), 2005. doi: 10.1175/MWR2906.1.
34. Stephan Rasp and Sebastian Lerch. Neural networks for postprocessing ensemble weather forecasts. *Monthly Weather Review*, 146(11):3885–3900, 2018. Publisher: American Meteorological Society.
35. Michael Scheuerer, Matthew B Switanek, Rochelle P Worsnop, and Thomas M Hamill. Using artificial neural networks for generating probabilistic subseasonal precipitation forecasts over California. *Monthly Weather Review*, 148(8):3489–3506, 2020. Publisher: American Meteorological Society.
36. Benedikt Schulz and Sebastian Lerch. Machine Learning Methods for Postprocessing Ensemble Forecasts of Wind Gusts: A Systematic Comparison. *Monthly Weather Review*, 150(1):235–257, January 2022. doi: 10.1175/MWR-D-21-0150.1. URL <https://journals.ametsoc.org/view/journals/mwre/150/1/MWR-D-21-0150.1.xml>. Place: Boston MA, USA Publisher: American Meteorological Society.
37. Benedikt Schulz, Mehrez El Ayari, Sebastian Lerch, and Sándor Baran. Post-processing numerical weather prediction ensembles for probabilistic solar irradiance forecasting. *Solar Energy*, 220:1016–1031, 2021. ISSN 0038-092X. doi: <https://doi.org/10.1016/j.solener.2021.03.023>. URL <https://www.sciencedirect.com/science/article/pii/S0038092X21002097>.
38. Nitish Srivastava, Geoffrey Hinton, Alex Krizhevsky, Ilya Sutskever, and Ruslan Salakhutdinov. Dropout: A Simple Way to Prevent Neural Networks from Overfitting. *Journal of Machine Learning Research*, 15(56):1929–1958, 2014. URL <http://jmlr.org/papers/v15/srivastava14a.html>.

39. Bert Van Schaeybroeck and Stéphane Vannitsem. Ensemble post-processing using member-by-member approaches: theoretical aspects. *Quarterly Journal of the Royal Meteorological Society*, 141(688):807–818, 2015. Publisher: Wiley Online Library.
40. Stéphane Vannitsem, John Bjørnar Bremnes, Jonathan Demaeyer, Gavin R. Evans, Jonathan Flowerdew, Stephan Hemri, Sebastian Lerch, Nigel Roberts, Susanne Theis, Aitor Atencia, Zied Ben Bouallègue, Jonas Bhend, Markus Dabernig, Lesley de Cruz, Leila Hieta, Olivier Mestre, Lionel Moret, Iris Odak Plenković, Maurice Schmeits, Maxime Taillardat, Joris van den Bergh, Bert van Schaeybroeck, Kirien Whan, and Jussi Ylhäisi. Statistical postprocessing for weather forecasts review, challenges, and avenues in a big data world. *Bulletin of the American Meteorological Society*, 102(3), 2021. doi: 10.1175/BAMS-D-19-0308.1.
41. Simon Veldkamp, Kirien Whan, Sjoerd Dirksen, and Maurice Schmeits. Statistical postprocessing of wind speed forecasts using convolutional neural networks. *Monthly Weather Review*, 149(4):1141–1152, 2021.

Author contributions statement

P.M. developed and implemented the ANET variants, designed the evaluation, and analysed the results. J.M. provided consultation and interpretation of the method design and results especially in a meteorological context. J.F.P. provided mentorship and guidance throughout the entire development, implementation, and evaluation stages of this research. All authors wrote and reviewed the manuscript.

Additional information

Code access

The ANET1 code for model estimation and post-processed forecast generation is open source and accessible at the Github repository [4].

The ANET2 code (including all tested variants) for model estimation and post-processed forecast generations is open source and accessible at the Github repository [2].

The data used for training and testing is a part of the EUPPBench benchmark [8].

Competing interests

The authors have no competing interests.

Acknowledgements

We would like to thank EUMETNET for providing the necessary resources, enabling the creation of the EUPPBench benchmark and to our colleagues behind the benchmark, whose dedicated work lead to its realization.

This work was supported by the Slovenian Research Agency (ARRS) research core funding P2-0209 (Jana Faganeli Pucer).

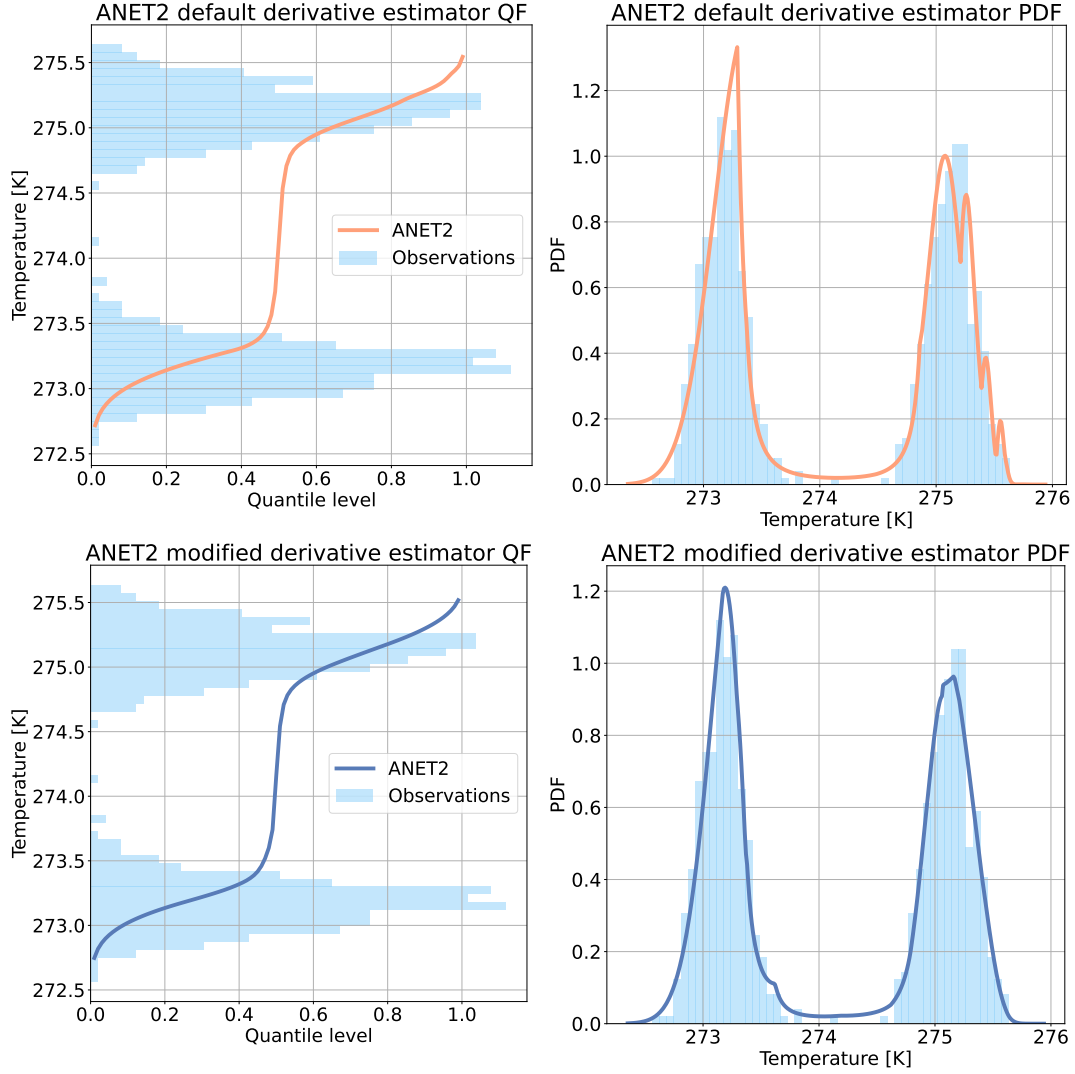


Figure 6. (Top): ANET2 with the default derivative estimator for the normalizing spline flow, as described by Durkan et al. [12]. (Bottom): ANET2 with the derivative estimation modification based on Gregory and Delbourgo [18]. QF denotes the plot containing the quantile function (inverse cumulative distribution function). The ANET2 variant with the modified derivative estimator on the bottom suppresses sharp non-linearities, resulting in more "natural" probability densities and a reduced amount of parameters that the model needs to predict. The observations are generated by sampling two normal distributions with equal variance at different mean temperatures.

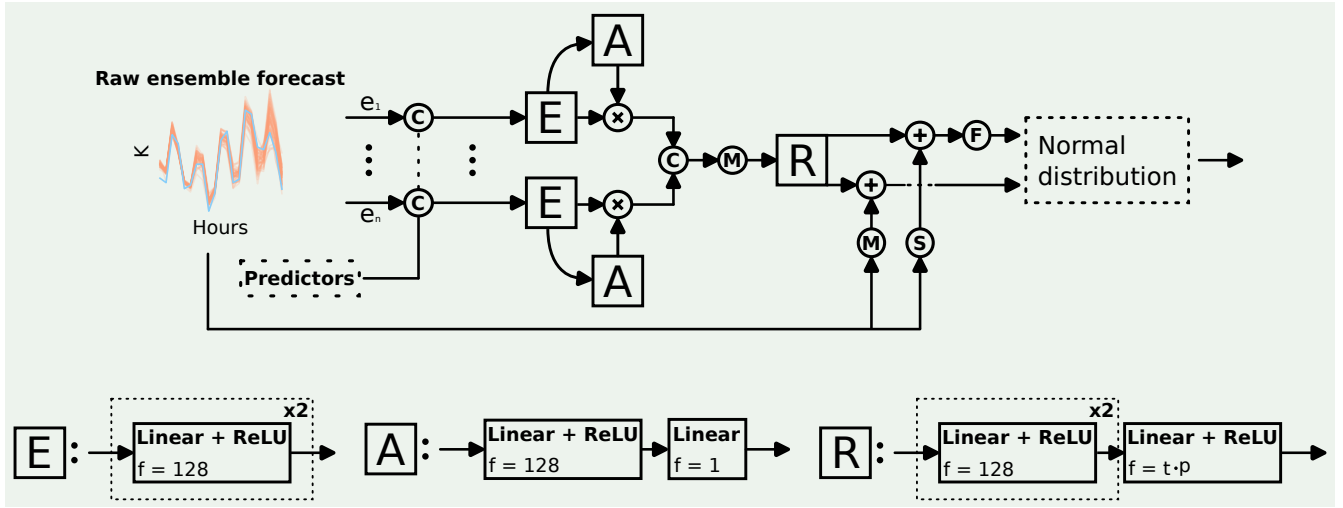


Figure 7. The neural network architecture of ANET1. The parameter f denotes the number of features in a dense layer. The parameters t and p denote the lead time and the number of per-lead-time parameters required by the normal distribution model. The circular blocks denote the following operations: M and S the ensemble forecast mean and standard deviation, X the element-wise product, C concatenation operation, and F the softplus activation [10]. The square blocks denote the following operations: E corresponds to the shared forecast encoder block, A corresponds to the dynamic attention block, and R corresponds to the regression block. The variable e_i denotes the i -th ensemble member in the forecast.

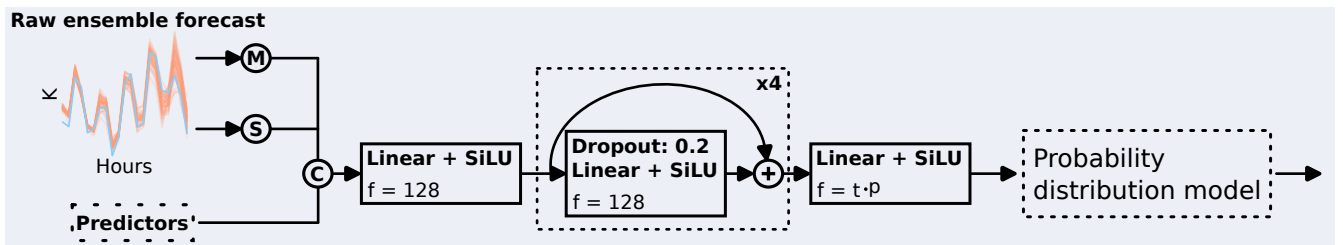


Figure 8. The neural network architecture of ANET2. The parameter f denotes the number of features in a dense layer. The parameters t and p denote the lead time and the number of per-lead-time parameters required by the normalizing flow. The circular blocks denote the following operations: M denotes the computation of the ensemble forecast mean, S block denotes the computation of the standard deviation of the ensemble forecast, and C denotes a concatenation operation.